

Algorithmic Method for Decorrelating a Bottom Signal and Structural Noise during Thickness Gauging of Large Items using Ultrasonic Phased Arrays

Vladimir K. Kachanov, Igor V. Sokolov, Alexey A. Sinitsyn* and Roman V. Kontsov

Moscow Power Engineering Institute (National Research University), Russia;
kachanovvk@mail.ru, sokoloff_igor@mail.ru, c.i.n@mail.ru, kontsovrv@mail.ru

Abstract

Background/Objectives: The article discusses problems of isolating signals from the structural noise correlated with a sounding signal using the ultrasonic echo method of measuring the thickness of large items with complex structure. **Methods:** The article demonstrates that in addition to spatial decorrelation of the bottom signal and the interference correlated with it, it is possible to use algorithmic decorrelation by using phased arrays and the signal processing algorithm which searches for the reflecting planes. **Findings:** Preliminary spatial correlation of the "useful" signal from structural noise is a condition for signal isolation. Measurement of the thickness of large, complexly structured concrete items is used to demonstrate that the use of the "focusing on a plane" algorithm will improve the bottom signal/structural noise ratio and thus increase the measurable thickness of the concrete items. **Applications/Improvements:** The use of the algorithm, "focusing on the plane" in modern thickness gauges and scanners applied for monitoring concrete structures can significantly increase the reliability and accuracy of defect detection.

Keywords: Focusing on a Spot, Focusing on a Plane, Structural Noise, Tomography, Ultrasonic Phased Array

1. Introduction

During Ultrasound (US) monitoring of concrete structures two similar problems often occur: the task of measuring the thickness of items with a known speed of US signal dissemination in concrete and the task of determining the ultrasound speed in concrete in items with a known thickness. Since the speed of US oscillations is unequivocally linked to the material strength, then according to Russian¹ and American standards², the speed of ultrasound in concrete determines its strength. These same standards determine that due to the high frequency-dependent damping of US oscillations in con-

crete relatively low frequencies (about 100 kHz and lower) should be used, and the thickness of concrete items should be measured by the shadow method which requires two-way contact with the item on test samples 15–20 cm thick. This same shadow method is recommended also for measuring ultrasound speed in large concrete items, and for greater thickness the standards recommend determining the speed of longitudinal waves in concrete from the measured surface wave, despite the fact that the US oscillation speed on the surface and inside the item may be very different. The possibility of measuring the speed (thickness) by echo-impulse method is not considered here due to the relatively low sensitivity of the echo method.

*Author for correspondence

The main reason for the low sensitivity of the echo method is that the US signal in the echo method passes two times faster than in the shadow method. If the US signals are very weak in the concrete³ the echo signals A_{21}, A_{22}, A_{23} from defects 1, 2 and 3 in Figure 1 could therefore be below the sensitivity threshold of the flaw detector $U_{\text{threshold}}$. The US signal is weakened in concrete in addition to absorption because of ultrasound scattering on the structural components (gravel grains). Structural Noise (SN) develops here. It is a series of multiple reflections of the sounding signal from the gravel grains which restricts the use of the echo method to monitor concrete items⁴.

The diagram of formation of structural noise during echo monitoring is shown on a simplified diagram in Figure 1 where the linear size of the item (1) and the time diagrams (A-scans) are superimposed in conventional scale. Figure 1b depicts the echo signals from defects and from the structural components which are presented as short video impulses for simplification. Multiple re-reflections of the echo signals on the structural com-

ponents, the radio-impulse nature of the signals and a lot more were not taken into account in this case. Despite the simplified nature of the SN depiction, the diagrams in Figure 1b and 1c show the real problem which arises during monitoring of concrete items: the sounding signal reflected from the numerous structural irregularities creates an interference, Structural Noise (SN), which masks the reflection from the defects. The SN level depends both on the gravel grain size \bar{D} , its quantity, packing density, and the signal parameters (frequency, duration of the impulse). A high SN level is observed in materials where the size of the structural irregularities \bar{D} is comparable to wavelength λ (with $\bar{D}/\lambda \rightarrow 1$). The SN level is low for materials with relatively small size of irregularities. Therefore, when monitoring items made of structural metals, the frequency of the US sounding signal is selected so that condition ($\bar{D} \ll \lambda$) is met while simultaneously ensuring the requisite resolution of the monitoring. A feature of concrete is that even at low ultrasound frequency ($f_0 \approx 100$ kHz) the extent of the US wave in the concrete ($\lambda \sim 4$ cm)

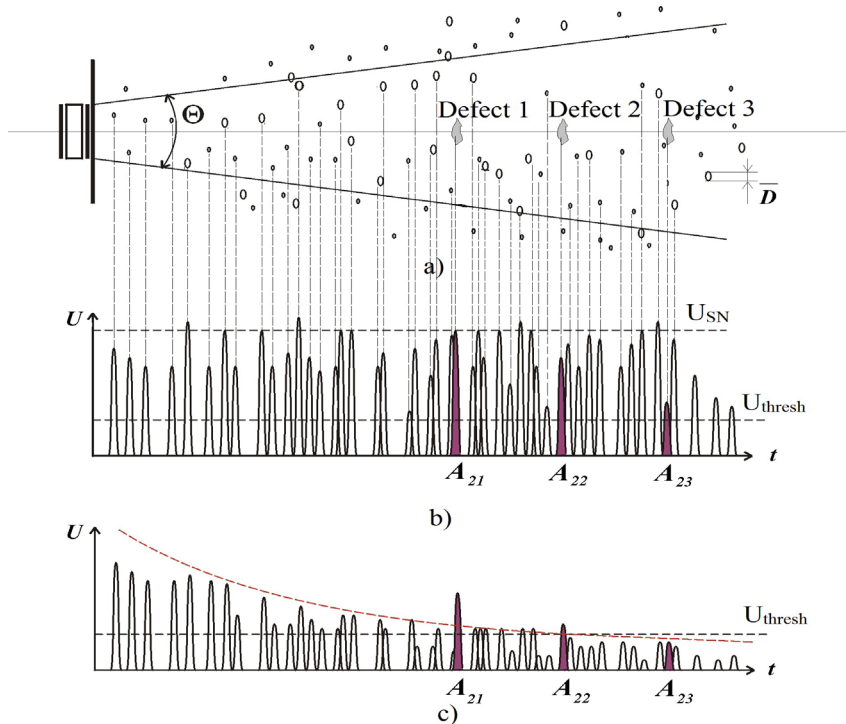


Figure 1. Conventional diagram of SN formation in an item with $\bar{D} \sim \lambda$: (a) Diagram of monitoring; (b) Echo signals from defects and from the structure without consideration for damping; c – with consideration for ultrasound damping.

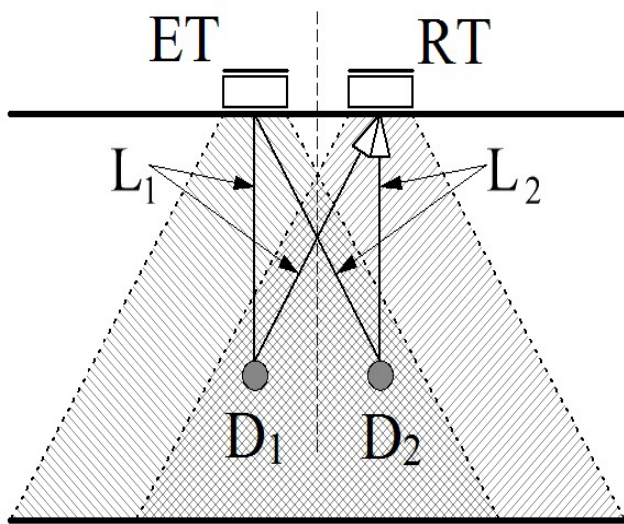


Figure 2. Ambiguous determination of the defect coordinates due to wide directional pattern of the transformers during US LF echo monitoring.

is comparable to the gravel grain size \bar{D} . A drop in the signal frequency below 100 kHz leads to a number of uncharacteristic problems during high-frequency monitoring of metal items:

First, resolution deteriorates and measurement accuracy drops as frequency is reduced. This circumstance does not permit the sounding signal frequency to fall below 50 kHz, although at such frequencies the US wavelength in concrete will be greater than the gravel dimensions ($\lambda > \bar{D}$) and structural noise diminishes.

Second, in a transformer with finite aperture D a drop in frequency increases the opening angle of the directional pattern (DP) $\theta \approx \arcsin \lambda/D$. Consequently, structural noise increases since the number of reflectors participating in SN formation rises. Additionally, emission directivity declines so that it is difficult to determine the azimuth coordinates of defects D_1 and D_2 shown in Figure 2 located in the area of joint directional pattern of the emitter (ET) and receiver (RT).

2. Methods

Since the problem of structural noise during monitoring of structural material items can be resolved by selecting

the optimal sounding signal frequency, the majority of traditional US monitoring instruments do not have special measures to isolate the “useful” signal from the SN. Moreover, if structural interferences appear, a number of instruments do not provide for a threshold limiter which cuts off interferences lying below the threshold level $U_{\text{threshold}}$. However, when monitoring such complex structural materials as cast iron, bronze and concrete the signals have to be isolated from the structural noise.

The MEI has proposed a solution to this problem based on spatial separation (decorrelation) of the signal and interference^{5,6}. Since SN is generated by the sounding signal, its spectrum is similar to the sounding signal spectrum. In other words, structural noise was correlated with both the sounding signal and the signal reflected from the defect. In order to isolate the “useful” signal from the correlated interference, the signal and the interference should be decorrelated. Such decorrelation is possible using temporal or frequency separation of signals⁷, however the most promising results are obtained when spatial separation of signals is used (use of multichannel monitoring methods)^{8,9}.

Figure 3 shows a simplified Signal Spatial Processing (SPP) system which explains the algorithm for isolating the “useful” echo signal (echo signal from a defect or

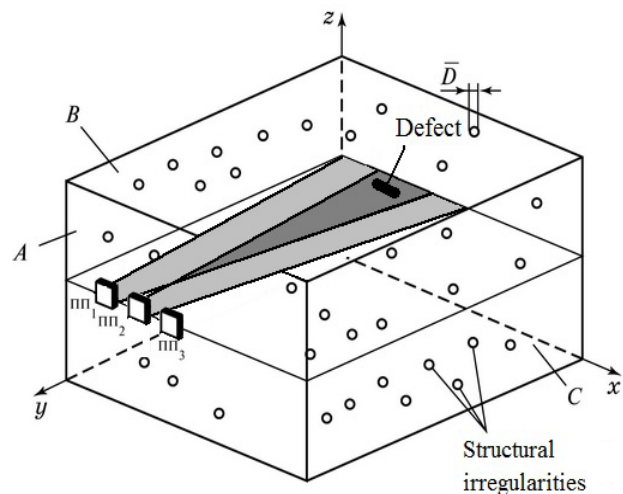


Figure 3. Simplified system of US signal spatial processing to isolate “useful” echo signals from SN using PET.

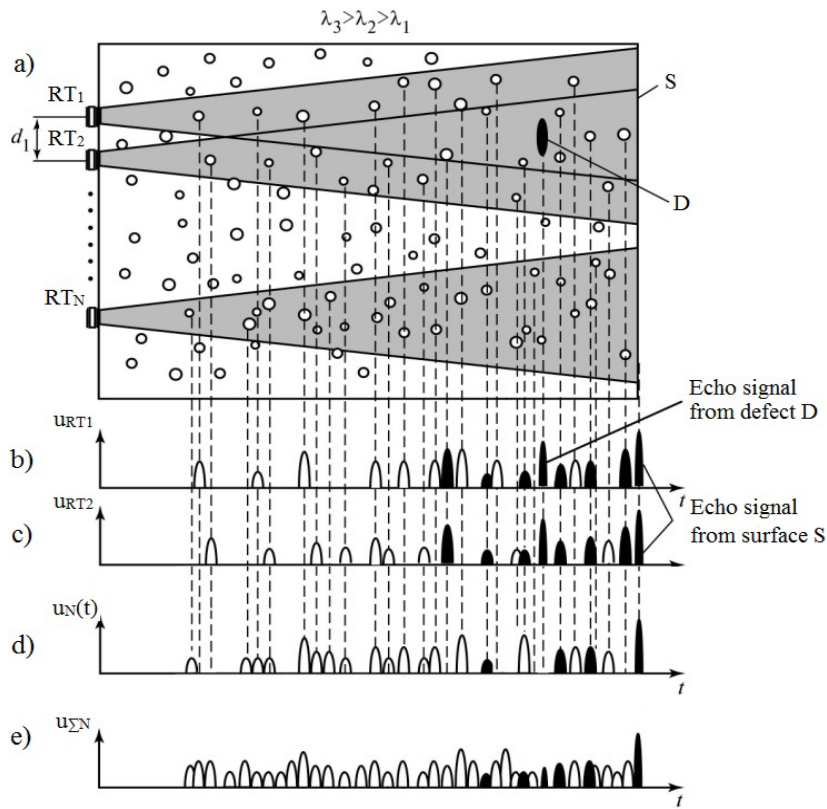


Figure 4. Simplified PVOS using PET with wide DP: a – formation of SN during multichannel processing; b – d – echo signals from structure and from defect in 1,2...N-rd channels; e – summary signal in N channels.

bottom signal) from SN. Spatial processing is generally done using N receiver transformers $RT_1 - RT_N$ which are spatially separated by distance d , but for simplification Figure 3 only shows three reception transformers RT_1 , RT_2 and RT_3 . The shading there also marks the cutting of the item by a plane passing through the reception transformers.

If the transformers have wide directional patterns, the defect is located in the visual field of all three transformers $RT_1 - RT_3$. Different acoustical irregularities in this case fall into the acoustical field of different transformers. As a result of spatial separation of the transformers, the time delays in the echo signals from the defect and from the bottom of the item on the diagrams in Figure 4b, c and d are the same for all the transformers, while the time delays

in the echo signals from the structural irregularities differ and have random values. In this case there is decorrelation of the structural noise signals shown as structural noise signals with a Function of Mutual Correlation (FMC) $\neq 1$ arriving at neighboring sensors. Maximum decorrelation is ensured if the neighboring transformers are placed at a distance called the correlation radius $d = r_k$, in which $FMC \leq 0.2-0.1^2$. The signals of neighboring spatial channels are then added (accumulated). If there is a bottom signal in each of the channels, then during accumulation of N implementations the amplitude of the “useful” echo signal rises by N times and the SN level no more than by \sqrt{N} times, resulting in a higher “useful” Signal/Structural Noise (S/SN) ratio by \sqrt{N} times.

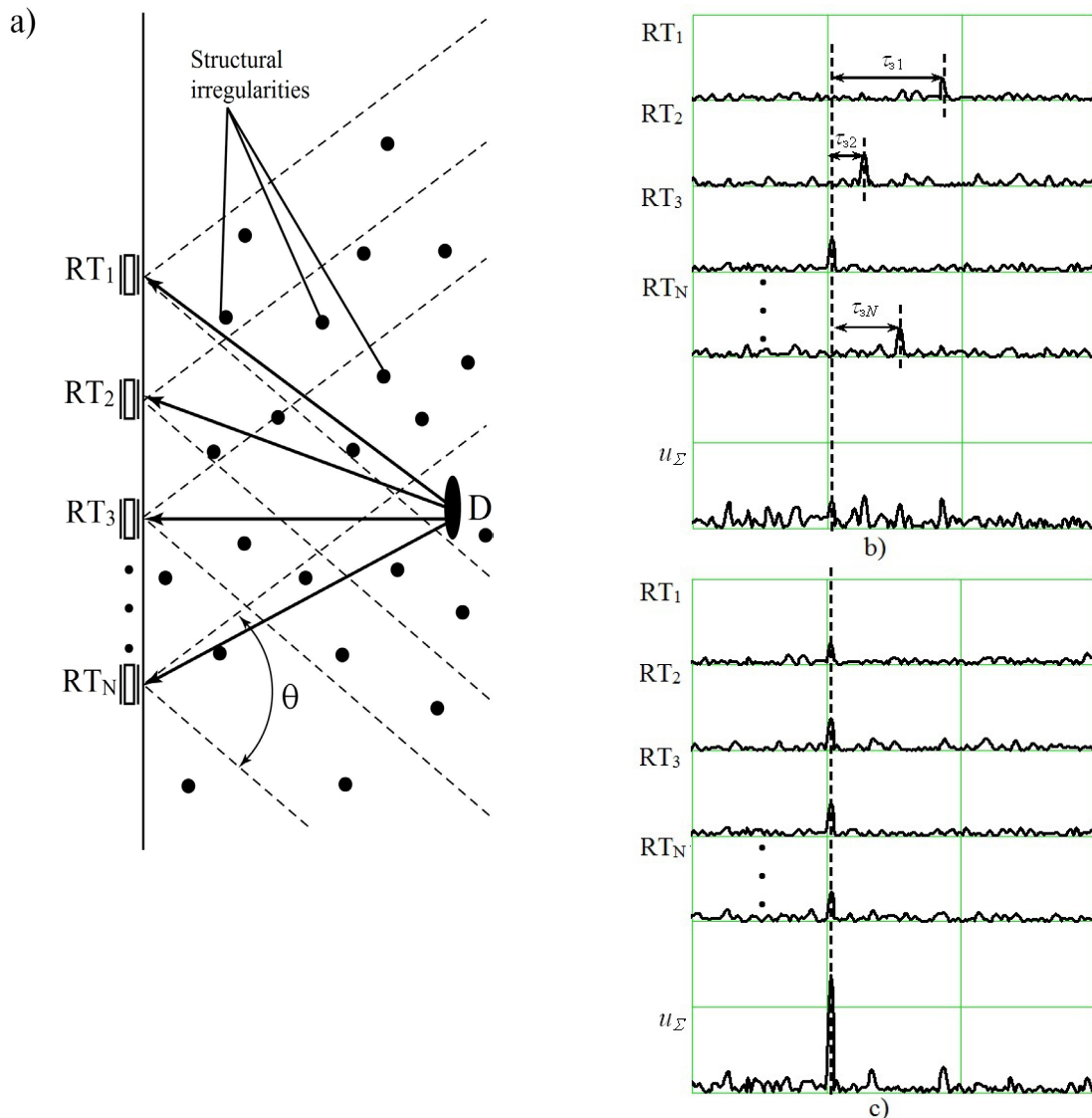


Figure 5. Simplified system of PVOS “focusing on a spot”: (a) System of experiment; (b) US echo signals on antenna components without signal phasing; (c) US echo signals on antenna components after echo signal phasing.

Spatial decorrelation can be performed both by moving one reception transformer over the item surface, and using a composite transformer, consisting of N independent reception transformers RT_1-RT_N with varying topology. The US linear Phased Array (PA) which is a set of transformers arranged on one line at distance $d \approx \lambda/2$ could also be called such composite transformer.

The PA has been widely used in recent years for imaging of concrete items. The PA operating principle is that they focus US signals on each spot in space shown Figure 5. Then the entire item is “scanned” in sequence and a two-dimensional image of the item is constructed from the set of echo signals from each spot. Each processing algorithm of the signals which arrived at all PA compo-

nents can be called a “focusing on a spot” algorithm. It was used to resolve the problem of unequivocal determination of defect coordinates during low-frequency monitoring. Additionally, the use of this algorithm ensures signal spatial processing, and at the same time, isolation of the “useful” signal from the SN.

In fact, N transformers $RT_1 - RT_N$ in Figure 5a (in all N implementations in Figure 5b) have echo signals from a defect, but in the summary signal U_{Σ} these reflections are separated in time and do not allow formation of a summary echo signal. Electronic focusing on a spot D is performed by selecting time delays $t_{d,1} - t_{d,N}$ so that all echo signals from defect D were combined in time and summed in phase, forming the maximum echo signal U_{Σ} at the time corresponding to the minimum delay $t_{d,3}=0$ (U_{Σ} in Figure 5c). If it is assumed that the SN in neighboring implementations (on neighboring transformers RT_1, RT_2, RT_3 , in Figure 5b) are very correlated, then in Figure 5c after “combination” of these implementations a new time distribution of CN is formed in which the structural noise is decorrelated in the neighboring channels. After compensation for time delays and summation of N echo signals the S/CN ratio increases. Thus, simultaneously with detection of the echo signal from the defect the “useful” echo signal from the SN is also isolated.

The “focusing on a spot” algorithm to be used in essentially all US imaging improves the S/CN ratio. However, it is precisely this algorithm which also limits the sensitivity of monitoring concrete items¹⁰. In fact, the “focusing on a spot” method is aimed precisely at the image of “spot” reflectors which allows precise detection of “spot” objects (defects) and good revelation of irregularity in the “spot” structure. This is precisely why the detected and revealed “spot” components in the structure (gravel grains in concrete) create on the concrete item image shown in Figure 6a a background (light green spots) masking the “useful” signal from the defect shown in Figure 6b.

The “focusing on a spot” algorithm here does not produce a clear image of the reflecting plane (bottom of item) as explained in Figure 7, where emitted signals $A_{and1} - A_{and5}$, lying within the transformer DP limits are shown for each of the US PA transformers. If the SAFT algorithm is used, these signals during mirror reflection from different spots on the plane fall onto different PA reception components. The echo signals reflected from the various plane spots in this case may fall both on the 5 PA components (for signals reflected from spot C), and only on 3 components or on 1 component (for a signal reflected from spot B). Signals reflected from spot A do not fall at all on any PA component.

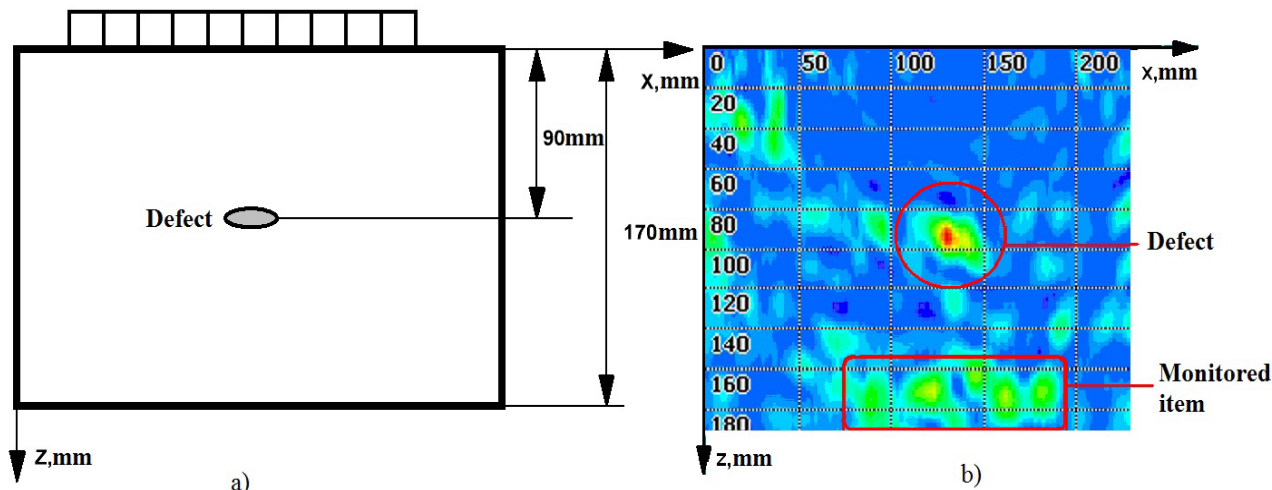


Figure 6. US imaging of concrete item with the spot reflecting object: (a) Monitoring system; (b) Item image.

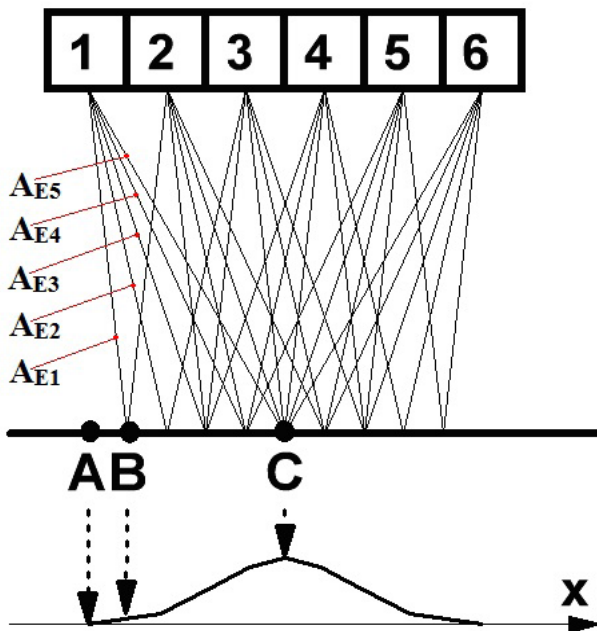


Figure 7. The effect of forming a “blurred” image of the reflecting surface.

Therefore in the resulting image, spot C will contribute the most to constructing the plane image: the maximum amplitude (b) will correspond to it. Spot B will correspond to the “spot” on the image, the amplitude of which is 3 times less, while spot A will have altogether zero amplitude. Consequently, the image of the bottom plane in Figure 6b when the “focusing on a spot” algorithm is used a blurred “section” is obtained with amplitude maximum in the middle and smoothly diminishing amplitude further from the antenna center.

The “focusing on a spot” algorithm, designed to reveal “spot” objects, thus reveals well the reflections from structural irregularities (gravel grains), forming structural noise, but gives a blurred image of the reflecting surfaces. In total these two qualities of the “focusing on a spot” algorithm limit the sensitivity of US imaging units operating in the mode of measuring the thickness of concrete items: the high level of structural noise does not allow an unclear image of the item bottom to be distinguished¹⁰ and restricts the reliably measured thickness of a concrete item.

3. Results

In order to reliably find the reflecting surfaces (planar defects, bottom surfaces, etc.) we developed a “focusing on a plane” algorithm¹¹ which determines the spatial coordinates of planes (distance from the PA to the plane, angle of inclination of the plane to the PA).

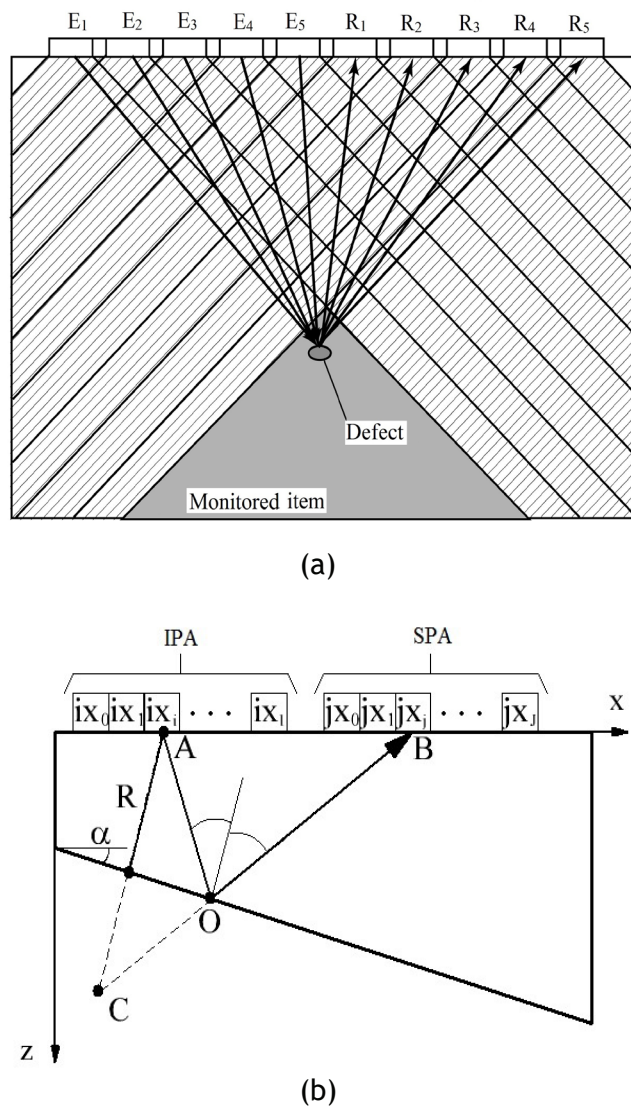


Figure 8. US PA System with spatially separated emitting and reception parts; (a) system of acoustic channel for one of the pairs of transformers to determine spatial coordinates of a planar reflector for the “focusing on a plane” algorithm (b).

The operation of the “focusing on a plane” algorithm is explained for a separately-combined PA (Figure 8a) consisting of $I = 5$ emitting and $6[J] = 5$ reception PET. As a result of searching all possible pairs of emitters and receivers, $I \times J$ of flaw patterns $U_{i,j,R,a}(t)$ are recorded with echo signals reflected from the reflector plane with coordinates R, α and passed the summary path $AO+OB=CB$ (Figure 8b). Formula (1) determines the delay times of the signals in the PA acoustic channels, considering which their coherent addition is performed.

$$T_{i,j,R,a} = \frac{\sqrt{4R_0^2 + (ix_i - jx_j)^2 + 4R_0 \cdot (ix_i - jx_j) \cdot \sin(\alpha)}}{C} \quad (1)$$

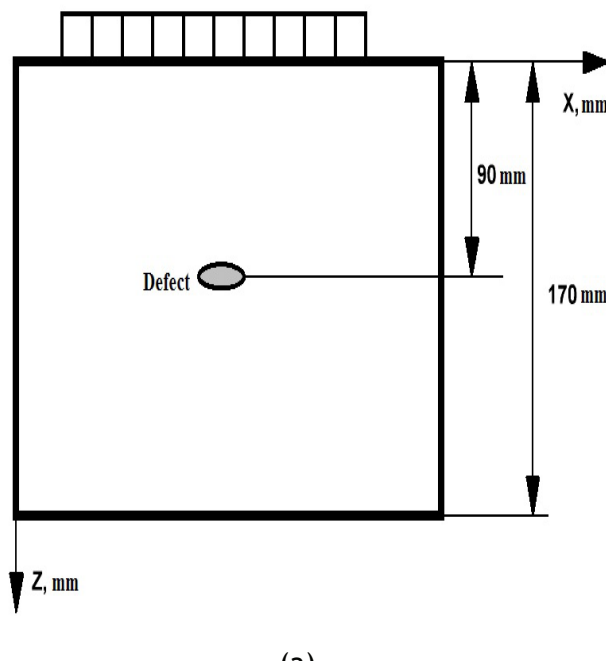
where R_0 – the shortest distance from the E to the reflecting plane.

The subsequent search of paired combinations of possible coordinate values of the planar reflector (R, α) permits formation of a two-dimensional matrix of amplitudes

of coherently summed signals. For each pair combination the summary signal $SS(R,a)$ is depicted by a colored mark at the spot with coordinates R,a . The color coding of amplitudes SS forms an image of the item on which the plane image is presented in the form of a brightness mark, the color of which is determined by the amplitude of the coherently summed echo signals of all $I \times J$ of the PA channels.

Figure 9 shows the results of determining the coordinates for the bottom of a concrete item (Figure 9a) with thickness $R = 170$ mm having a hole 25 mm in diameter at a depth of 90 mm using US LF broad-band PA. The band of working frequencies PET of the PA is $\Delta f = f_B - f_H = 275 - 125$ kHz = 150 kHz. The mean frequency of the employed signal with linear frequency modulation (LFM) was $f_0 = 200$ kHz, frequency deviation $\Delta f \approx 80\%$, amplitude 10 V.

The image of the plane provides an unusual picture for classic imaging of the internal structure of the monitored item, and only notes the probable existence of a planar reflector with coordinates R and a , which also determined



(a)

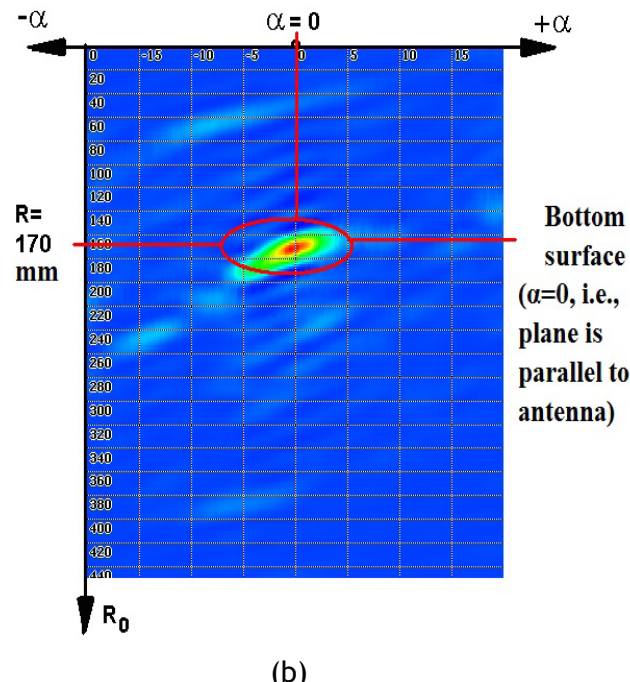


Figure 9. Obtaining an image of a plane using the “focusing on a plane” algorithm: (a) System of the experiment; (b) Image of plane using LFM of a signal with a mean frequency of 200 kHz.

the name of the image: “probability image” or “P-scan.” Coordinates ($R = 170$ mm, $a=0^\circ$) of the plane are determined by the red marker (by the spot). On the P-scan in this case there is no image of a cylindrical hole 25 mm in diameter. This indicates that the algorithm for detecting planar reflectors is insensitive to “spot” reflectors. At the same time, on the P-scan there are local light green spots, similar to the image of the internal structure of the item on the image in Fig. 6, b which used the algorithm “focusing on a spot.” However, Fig. 9, b uses the algorithm “focusing on a plane,” therefore the externally similar light green spots indicate the presence not of “spot,” but of “planar” reflectors.

4. Discussion

The mechanism for detecting such planar reflectors is explained in Figure 10. A concrete item contains numerous structural components which could be randomly

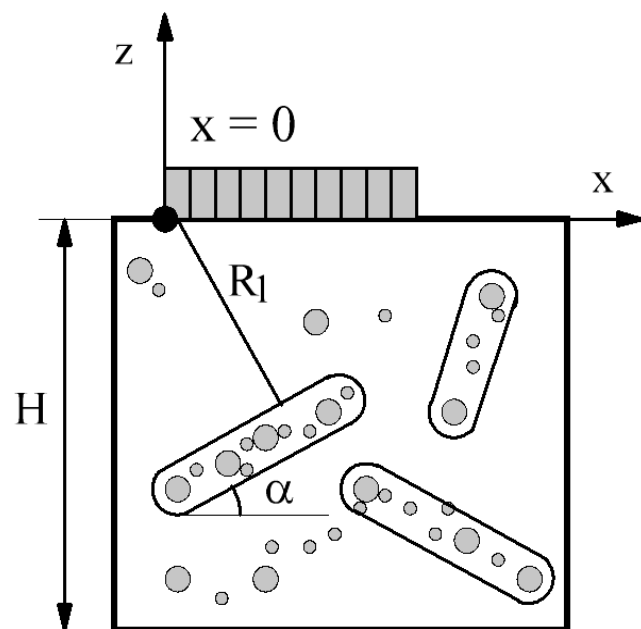


Figure 10. Mechanism for detecting “phantom planes”.

“arranged” in the form of planes with random coordinates R[3] and a (we called them phantom planes and encircled by contours). The nature of reflection of US waves from such phantom planes will be diffuse, but a part of the reflections from them will enter the US PF with delays corresponding to this flat phantom reflector. The amplitude of the interference spots on the P-scan depends on the shape, size and number of such phantom planes.

The “focusing on a plane” algorithm which detects predominantly planar reflectors “does not notice” spot reflectors. At the same time it enables to significantly reduce the masking effect of structural noise which is the aggregate reflection from spot reflectors, and improves the sensitivity of finding flat objects.

This is confirmed experimentally: Figure 11 shows the results of measuring a concrete item $R=200$ mm with filler sized $\bar{D}=15$ mm by the two algorithms with changes in the parameters of the LFM signal. In both cases the reflecting plane is detected, in both cases the plane is visible as a clear orange spot on the background of reflections from the structural components. However, it should be distinguished that in Figure 11 this spot corresponds to the image of the bottom of the item on the structural noise background, while in Figure 11b this is an image of the plane on the P-scan. The level of interference in this case (light green spots) is significantly lower when the “focusing on a plane” algorithm is used.

Figure 12 shows the results of measuring a concrete item 400 mm thick. As thickness increases, the “focusing on a spot” algorithm no longer permits detecting the item bottom due to the high level of SN: the light green spot in Figure 12a corresponding to the bottom plane located at a distance $R=400$ mm is barely noticeable on the background of interferences. The SN intensity here (bright yellow and orange spots) is significantly higher. When the “focusing on a plane” algorithm is used (Figure 12b) the bottom coordinates are determined unequivocally by the bright red spot with coordinates ($R=400$ mm, $a=0^\circ$) on the background of light green interference spots.

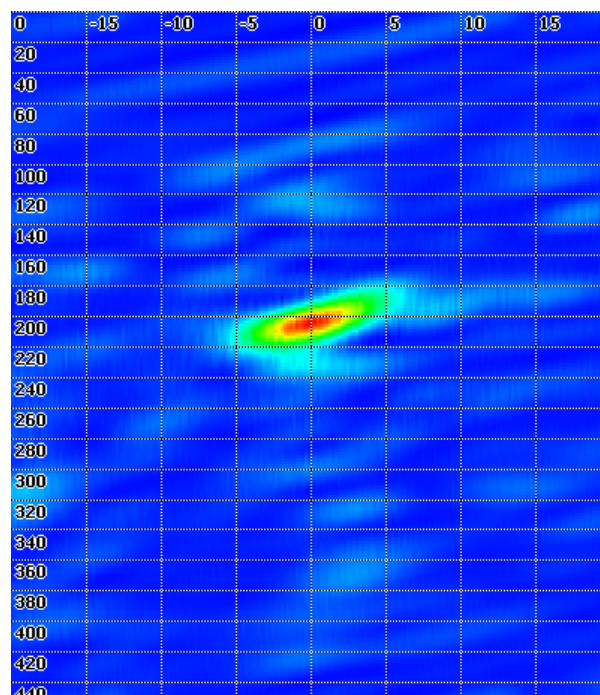
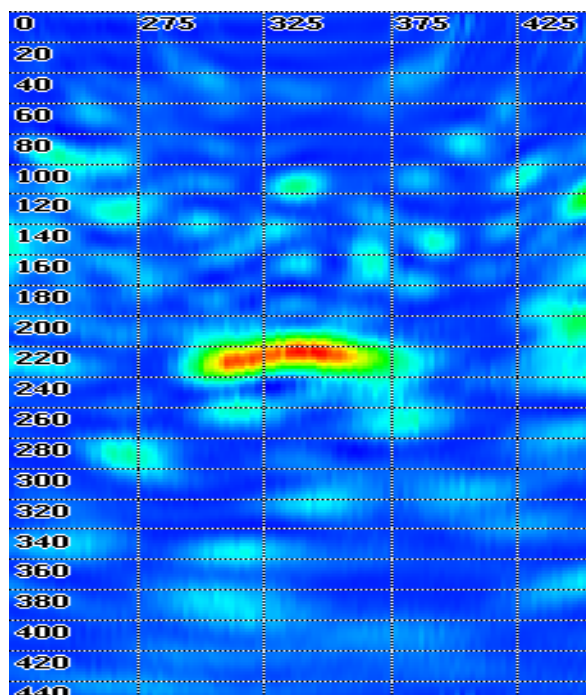


Figure 11. Results of finding a plane located at a distance of 200 mm from the US PA using the “focusing on a spot” algorithm (a) and the “focusing on a plane” algorithm (b).

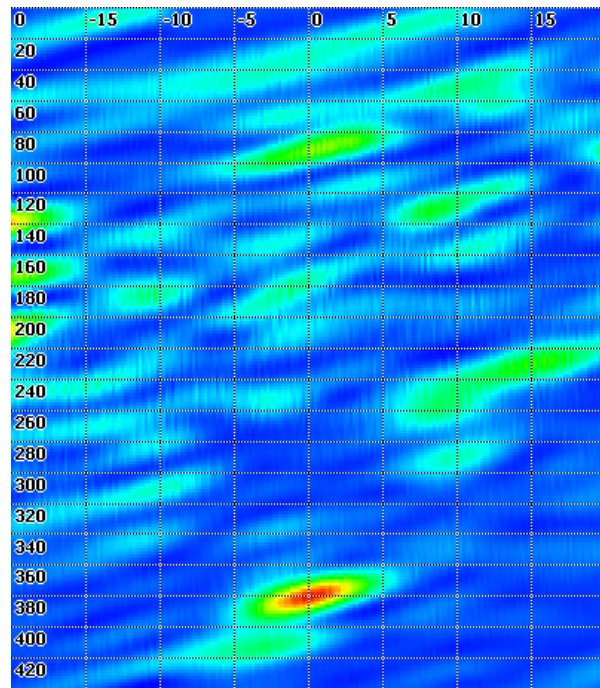
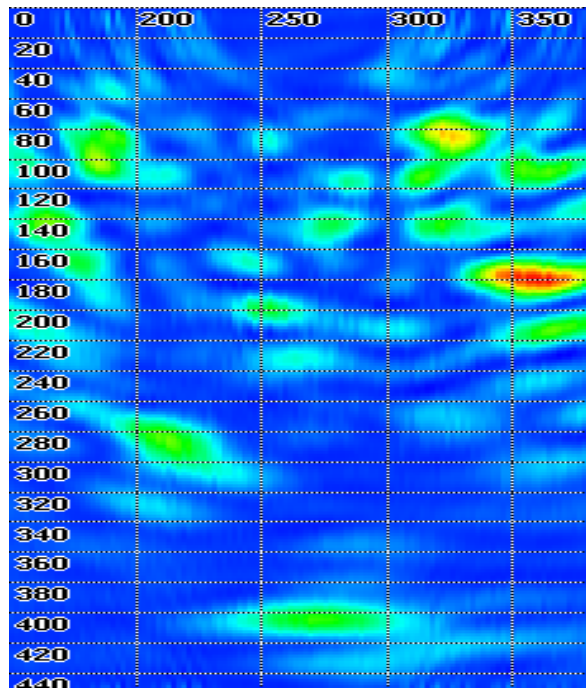


Figure 12. The results of detecting the reflecting surface located at distance of 400 mm from the US PA using the “focusing on a spot” algorithm (a) and the “focusing on a plane” algorithm (b).

5. Conclusions

Our developed spatial algorithm for processing ultrasound signals “focusing on a plane” is designed to measure the thickness of large concrete construction structures using phased arrays.

The “focusing on a plane” algorithm makes it possible to determine the distance to the reflecting surface R and the inclination angle of the reflecting plane.

The “focusing on a plane” algorithm does not make it possible to determine the presence of spot reflectors.

If the “focusing on a plane” algorithm is used, the algorithmic method of structural noise decorrelation is carried out (in the understanding of SN as an aggregate reflection from spot reflectors and “useful” signal). At the same time, the “focusing on a plane” algorithm ensures a higher signal/structural noise ratio.

During thickness measurement of concrete items, the “focusing on a plane” algorithm has greater sensitivity compared to the algorithm “focusing on a spot,” and at the same time it increases the reliably controllable thickness of complexly constructed concrete items.

6. Acknowledgment

The reported study was funded by RFBR and Moscow city Government according to the research project No. HP15-38-70046\15 “mol_a_mos”.

7. References

1. STO (standard organization) 36554501-009-2007 Betony. Ultrazvukovoj metod opredelenija prochnosti. [Concretes. Ultrasonic method for determining the strength]. 2007.
2. ASTM C 597. Standard test method for pulse velocity through concrete. Annual Book of ASTM Standards 4. 2002.
3. Kachanov VK, Sokolov IV. Issues of ultrasonic testing of extended complexly structured items with strong attenua-
- tion of signals. Russian Journal of Nondestructive Testing. 2007; 43(8):555-63.
4. Kachanov V K, Kartashev V G, Sokolov I V, Turkin M V. Problems of extracting ultrasonic signals from structural noise during inspection of articles produced from materials with complex structures. Russian Journal of Nondestructive Testing. 2007; 43(9):619-30.
5. Kartashev VG, Kachanov VK. Optimal allocation of signals against structural noise in ultrasonic testing. Russian Journal of Nondestructive Testing. 1992; 7:14-24.
6. Kachanov VK, Kartashev VG, Popko VP. Application of signal processing methods to ultrasonic non-destructive testing of articles with high structural noise. Nondestr Test Eval. 2001; 17:15-45.
7. Kachanov VK, Sokolov IV, Rodin AB. Frequency separation of signals and interferences in noise-immune ultrasonic testing of articles manufactured from complexly structured materials. Russian Journal of Nondestructive Testing. 2008; 44(11):747-61.
8. Kachanov VK, Kartashev VG, Sokolov IV, Voronkova LV, Rodin AB, Timofeev DV. Problems and features of spatiotemporal signal processing in ultrasonic testing of products manufactured from complexly structured materials. Russian Journal of Nondestructive Testing. 2010; 46(4):235-48.
9. Kartashev VG, Kachanov VK, Shalimova EV. The fundamentals of the theory of spatiotemporal signal processing as applied to problems of ultrasonic flaw detection of articles from complexly structured materials. Russian Journal of Nondestructive Testing. 2010; 46(4):249-57.
10. Kachanov VK, Sokolov IV, Turkin MV, Shalimova EV, Timofeev DV, Konov MM. Features of applying the method of focusing to a point in ultrasonic testing of products manufactured from complexly structured materials. Russian Journal of Nondestructive Testing. 2010; 46(4):258-69.
11. Kachanov V K, Sokolov IV, Timofeev DV, Turkin MV, Shalimova EV. Detection of reflecting planes in ultrasonic tomography of concrete building structures. Russian Journal of Nondestructive Testing. 2010; 46(5):342-9.